



Structural And DC Conductivity Studies of Samarium Substituted Ni-Zn Ferrites

KEYWORDS

Ferrites; IR Spectra; DC Electrical conductivity; electron hopping; Activation energy.

G J Shankaramurthy

Department of Physics, University B D T college of Engineering, Davangere 577 004 Karnataka, India.

H S Jayanna

Department of Physics, Kuvempu University, Shankaraghatta 577 451, Karnataka, India.

ABSTRACT

Polycrystalline ferrites having the general formula $Ni_xZn_{1-x}Fe_2-ySm_yO_4$ ($x = 0.00, 0.25, 0.50, 0.75, 1.00$; $y = 0.00, 0.05, 0.10$) were prepared by standard ceramic method. The samples were characterized by XRD techniques. The single-phase spinel formation of ferrites was confirmed by X-ray diffraction technique. The IR spectra show four absorption bands in the frequency range 300 cm^{-1} to 800 cm^{-1} . The first band ν_1 around 600 cm^{-1} and second band ν_2 around 400 cm^{-1} were assigned to the octahedral metal complexes. The other low frequency bands ν_3 assigned to the octahedral metal-oxygen complexes, and ν_4 related to some type of vibrations of the tetrahedral of octahedral metal oxygen complexes. The DC electrical conductivity of the palletized samples was measured by two-probe method in the temperature range 300K to 840K . The electrical conductivity in ferrites can be explained on the basis of exchange of electrons between ions of the same element that are present in more than one valence state, distributed randomly over equidistant crystallographic lattice sites. The electrical conductivity in ferrites to be due to the simultaneous presence of both Fe^{2+} and Fe^{3+} ions and due to electron hopping between Fe^{2+} and Fe^{3+} ions of octahedral sites. The electrical properties of ferrites are affected by the distribution of cations in sites by magnetic and non magnetic substitutions, the amount of Fe^{2+} ions present, sintering conditions, grain size and grain growth. The experimental results reveal that the DC conductivity increases as temperature increases and as the Zn^{2+} and Sm^{3+} ion content decreases. The electrical conduction mechanism in these ferrites is on octahedral sites. The activation energy for ferrimagnetic region is lower than in paramagnetic region. The addition of Sm^{3+} impedes conduction in samples. Thus, the activation energy is higher for Sm^{3+} substituted samples than those for the corresponding undoped samples in both the regions.

1. Introduction

The ferrites have attracted much attention because of their interesting electrical and magnetic properties. The properties of ferrites depend on their chemical composition, cation distribution and method of preparation [1]. The structure is based around a face centered cubic array of oxygen atoms with cations filling either the tetrahedral (A-sites) or octahedral (B-sites) interstices within this array. Ferrites having spinel structure are ferrimagnetic and have semiconductor properties of type n or p [2]. The factors specific to semiconductor with the super exchange interaction will be low carrier mobility, increase with temperature for the conductivity of the hopping type and correlation with magnetic state of the materials. The conduction mechanism in ferrites is quite different from that of semiconductors. In ferrites the temperature dependence of mobility affects the conductivity and the carrier concentration is almost independent of temperature [3]. The electrical properties of ferrites are affected by the distribution of cations on A and B sites, magnetic and non-magnetic substitutions, the amount of Fe^{2+} ions present, sintering conditions, porosity, presence of impurities and microstructure. Electrical conductivity can be increased by mixing small amount of foreign oxides in low conductivity composites. The ferrite which contain iron in excess show n-type conduction and those with iron deficiency show p-type conduction. The substitution of small amounts of the rare earth ions may bring about important modifications in structure and electrical, magnetic properties of the ferrites. The substitution shifts the Curie point to lower temperature side and increases the resistivity. Many workers have studied the DC conductivity of Mg ferrites [4], Ni-Zn [5-7], Mg-Zn [8, 9], Ni-Mg-Zn [10], Mg-Ni ferrites [11] and rare earth element substituted Ni-Zn [12] and Cu-Cd ferrites

[13]. In the present communication we report the studies on the effect of Sm^{3+} substitution on structure and DC conductivity of Ni-Zn ferrites.

2. Experimental

A series of samples of the system $Ni_xZn_{1-x}Fe_2-ySm_yO_4$ ($x = 0.00, 0.25, 0.50, 0.75, 1.00$; $y = 0.00, 0.05, 0.10$) were prepared by usual ceramic method. The reagent grade NiO , ZnO , Fe_2O_3 and Sm_2O_3 were mixed stoichiometrically and pre-sintered at 1000°C for 20 hours in a furnace. The samples were pressed in to pellets by applying the pressure of 5-ton/cm^2 for 5 minutes. The pellets were sintered at 1100°C for 8 hours and furnace cooled to room temperature. The single-phase spinel formation of ferrites was confirmed by X-ray diffraction patterns obtained on Philips X' Pert PRO diffractometer using $Cu\ K\alpha$ radiation ($\lambda = 1.54056\text{ \AA}$). The DC electrical conductivity of the palletized samples were measured by means of two-probe method. The silver paste was applied on either side of the pellets for good ohmic contacts. The pellet was sandwiched tightly between two silver electrodes in a sample holder with the help of screws and kept in a cell. Then cell was placed in a furnace. A calibrated Chromel-Alumel thermocouple was used to measure the temperature of the sample. A suitable constant and low voltage (5 Volts) was applied across the pellet and the corresponding current through the sample was measured in the temperature range from 300K to 840K . The conductivity of all the samples were calculated using the relation,

$$\sigma = t / (\pi r^2 R)$$

Where t - thickness of pellet

r - radius of pellet

R - resistance of sample ($R = V/I$)

3. Results and Discussions

3.1 X- ray analysis

The analysis of X-ray diffraction pattern revealed that all the samples have single phase of spinel cubic structure. Typical diffractograms are presented in the fig 1-(a) and fig1-(b). The gradual decreasing trend in the lattice constant in due to replacement of smaller ionic radii of Zn²⁺ ions by larger ionic radii of Ni²⁺. The increasing in lattice constant is also due to the replacement of Fe³⁺ ions in the octahedral site by comparatively larger Sm³⁺ ions. The similar results have been reported for rare-earth element substitutions for Cu-Cd [14], Mg-Zn [15] and Ni-Zn [16, 17] ferrites. It was reported that Zn²⁺ ions strongly prefers to occupy the tetrahedral site [18, 19] while Ni²⁺ ions occupy the B sites. As Zn²⁺ ions are decreased by Ni²⁺ substitution, it leads to a migration of some Fe³⁺ ions from B-site to A-Sites, as a result tetrahedral radius decreases.

The X-ray density for each composition was calculated using the relation

Where Z is the number of molecules in a unit cell, M is the molecular weight of the sample, N is the Avogadro number and V is the volume of the unit cell for cubic system. It is found that the X-ray density decreases with increase of Zn²⁺ and Sm³⁺ substitution. The lattice parameter, radii of tetrahedral site and octahedral site and X-ray density increases as Zn²⁺ decrease. The results are summarized in the Table 1.

$$D = \frac{ZM}{VN} \text{ gm/cm}^3$$

3.2 IR Analysis

Infrared Spectra is useful to detect the presence of absorption or emission bands in the ferrites. Since the electric and magnetic properties of these materials are decisively dependent on the precise configuration of the atoms or ions in these structure. Generally four active infrared active infrared bands are reported in the range 200 cm⁻¹ to 1000 cm⁻¹. The high frequency band v1 is related to tetrahedral complexes and low frequency band v2 to octahedral complexes. The low frequency band v3 is due to divalent octahedral metal ion-oxygen complex. The fourth band v4 depends on the mass of the divalent tetrahedral cation and is related to some type of vibrations involving a displacement of tetrahedral cation. Ferrites possess the structure of mineral spinel that crystallizes in the cubic form with space group Fd3m-o7h.

In the present work, IR spectrum of Nix Zn1-x Fe2-y SmyO4 ferrite samples has shown the two strong bands. The band v1 near 600 cm⁻¹ arises due to tetrahedral complexes and v2 around 400 cm⁻¹, due to octahedral complexes. The difference in the two strong bands v1 and v2 could be related to difference in Fe³⁺-o²⁻ distances for A and B sites. The absorption bands for the ferrites are found to be in the expected range [20, 21]. The infrared spectra of samples are shown in the Fig.2 (a) to (f). It can be seen that the slight variation in v1 and v2 indicates that the method of preparation, grain

size and porosity can influence in locating the band position. The absorption band v1 doesn't show any splitting and hence the possibility of Fe²⁺ ions at A-sites is ruled out. The presence of Fe²⁺ ions on the octahedral sites of ferrites can cause splitting of absorption band v2. It can also observed that the intensity of the band v1 decreases with decreases in Zn²⁺ ion content with increase in Sm³⁺ and Ni²⁺. The splitting in v3 and v4 also increases with the increase in compositions of Sm³⁺ while the lower frequency bands of IR absorption spectrum continues to widen. The low frequency band v3 is due to divalent octahedral metal ion-oxygen complex. The fourth band v4 appears for all the composition (except for the composition x =0.00, 0.25, 0.50, 1.00, y=0.00 and x=0.50; y=0.05,) which depends on the mass of the divalent tetrahedral cation and is related to some type of vibrations involving a displacement of tetrahedral cation. The similar results have been reported for rare earth element substitution for cu-cd, Mg-Zn and Ni-Zn, Zn-Ni Mg ferrite [22]. The band positions are listed in the table (2).

3.3 Temperature dependence of electrical conductivity (σDC)

The variation of lnσ v/s 1/T for all the samples of the present system NixZn1-xFe2-ySmyO4 (x =0.0, 0.25, 0.50, 0.75, 1.00; y =0.10) are shown in the Figs 3(a) to 3(c). From these plots it is observed that the conductivity increases with increase of temperature for all the samples and shows a transition near curie temperature. At this temperature the material undergo transition from ferrimagnetic state to paramagnetic state. For x=0.00: Y=0.00, 0.05&0.10 graph is found to be a straight line. This suggests that these samples are paramagnetic in nature. The change in slope is observed near curie temperature due to change in conduction mechanism. The activation energies corresponding to paramagnetic and ferrimagnetic regions were calculated. The change in the activation energy is due to the splitting of the conduction and valance band below Tc, above the curie temperature the bands are degenerate for the spin direction [23, 24, 25]. Therefore a reduction in the activation energy is expected as the samples undergo transition from ferrimagnetic to paramagnetic state. Similar results were observed by Rane et al., [26]. The calculated values of critical temperature Tc, activation energies for paramagnetic and ferrimagnetic regions are listed in the Table 3.

The electrical conductivity in ferrites can be explained on the basis of exchange of electrons between ions of the same element that are present in more than one valence state distributed randomly over equivalent crystallographic lattice states (Fe³⁺↔Fe²⁺) [27]. The formation of small amount of Fe²⁺ ions is expected owing to evaporation of zinc during the sintering process [28]. The conduction in paramagnetic region is explained as impurity conduction, while that in the ferrimagnetic region is due to electron hopping between Fe²⁺ to Fe³⁺ on B site.

From the table it is observed that the activation energy for ferrimagnetic region is lower than in the paramagnetic region, which may be attributed to the effect of spin ordering. This is in agreement with the results of Irkin and Yurov [29].

From the table it is also observed that, the critical temperature increases with increase in Ni content and the critical temperature decreases for samarium substituted samples. The substitution of Sm³⁺ ion for Fe³⁺ ion at B-site

impedes conduction mechanism in the samples due to its stable valency. The substituted Sm^{3+} ion, whose 4f orbital is shielded with 5s and 5p orbital, occupy octahedral site and hence Sm-Fe, Ni-Sm interaction is weaker than Fe-Fe interaction. This suggests that the electron transfer can take place during the conduction process between Fe^{2+} and Fe^{3+} and not favoured the case between Sm^{3+} and Fe^{2+} ions. The activation energy for Sm^{3+} substituted samples is more than those for the corresponding undoped samples in both ferrimagnetic and paramagnetic regions. Similar results have been reported for Gd^{3+} substituted Cu-Cd ferrites [30]. Thus, higher the activation energy, lower the conductivity for Sm^{3+} substituted samples. The Curie temperature mainly depends upon the strength of A-B interaction.

3. 4 Compositional dependence of DC conductivity

Fig.4 shows the variation of DC electrical conductivity with composition. From the figure it is observed that the conductivity increases with decrease in Zn content. The increase in conductivity with decrease in Zn content can be attributed to the excess formation of Fe^{2+} ions since these ions may also be formed due to the evaporation of Zn during sintering process. At $x=0.75; y=0.05, 0.10$ the conductivity decreases due to overall decrease of Fe ion on Zn substitution. It is clear that Curie temperature increases with increase in Ni content.

The conduction in the ferrite is due to hopping of electrons among iron ions on octahedral sites. During this hopping, change in valency takes place. The rare earth ions having stable valency do not contribute electron hopping but provide impediment to the conduction process. This leads to the decrease in conductivity on Sm^{3+} substitution, the activation energy is found to be increased which may be the cause for decrease in conductivity.

4. Conclusions

The lattice parameter, site radii, and x-ray density increase as Zn^{2+} concentration increases. The DC electrical conductivity increases as temperature increases and as Zn and Sm content decreases. The activation energy in paramagnetic region is higher than in the ferrimagnetic region. Curie temperatures (TC) decrease with increase in Zn and samarium ion content. The activation energy for Sm^{3+} substituted samples both in ferri and paramagnetic region are higher than those for unsubstituted samples.

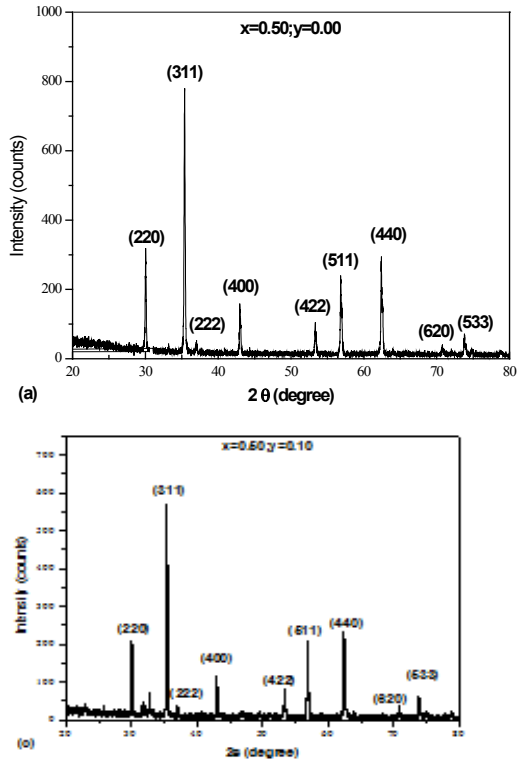
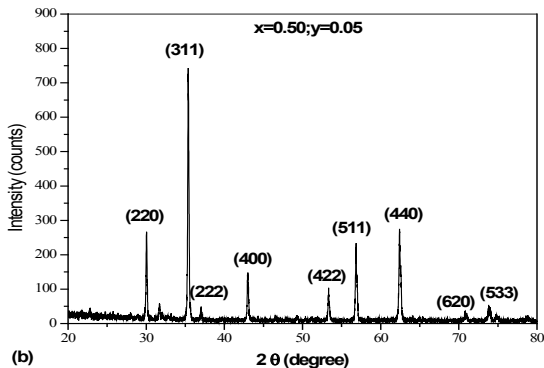
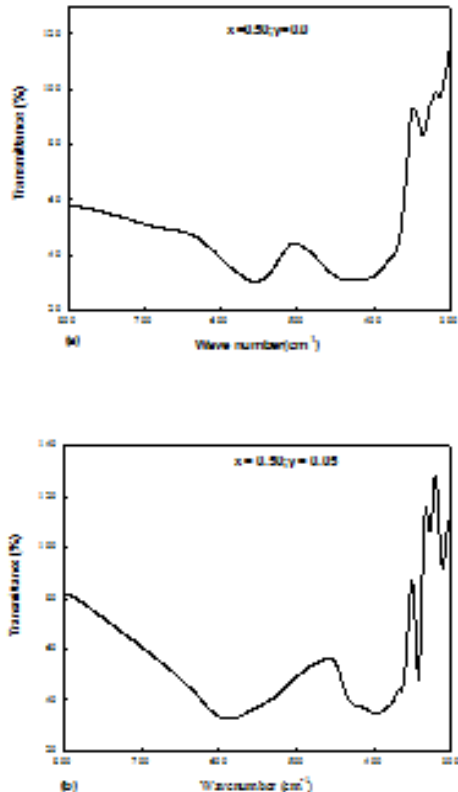


Figure 1.



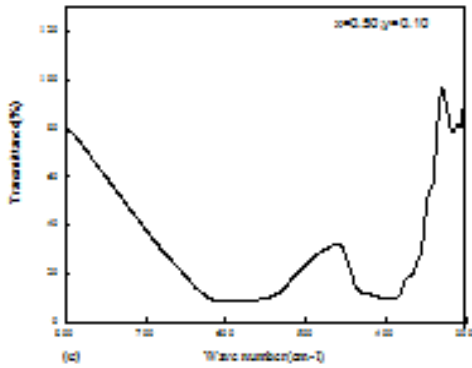


Figure 1. X-ray diffraction patterns of Zn_{1-x} Ni_xFe_{2-y}S_mO₄ ferrites with composition (a) x = 0.5; y = 0, (b) x = 0.5; y = 0.05 and (c) x = 0.5; y = 0.1

Figure 2. IR Spectra of Zn_{1-x} Ni_xFe_{2-y}S_mO₄ ferrites with composition (a) x = 0.4; y = 0, (b) x = 0.5; y = 0.05 and (c) x = 0.5; y = 0.1

Figure 3. Variation of DC conductivity with temperature of Zn_{1-x} Ni_xFe_{2-y}S_mO₄ ferrites with composition x = 0, 0.25, 0.50, 0.75, 1.00; (a) y = 0, (b) y = 0.05 (c) y = 0.1

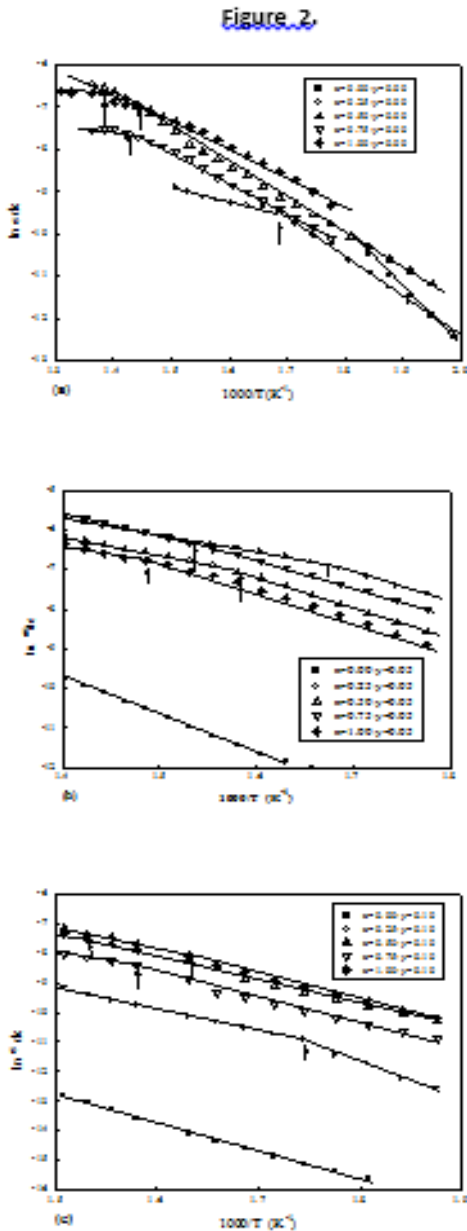


Figure 3.

Composition		Lattice parameter (Å)	r _A (Å)	r _B (Å)	X-ray Density (g/cm ³)
X	Y				
0.00	0.00	8.41	0.466	0.752	5.379
0.25		8.41	0.467	0.753	5.337
0.50		8.37	0.458	0.742	5.379
0.75		8.30	0.443	0.725	5.478
1.00		8.35	0.455	0.739	5.331
0.00	0.05	8.42	0.470	0.756	5.454
0.25		8.38	0.462	0.747	5.490
0.50		8.35	0.454	0.738	5.522
0.75		8.31	0.445	0.727	5.569
1.00		8.27	0.436	0.718	5.607
0.00	0.10	8.43	0.470	0.757	5.551
0.25		8.36	0.456	0.740	5.647
0.50		8.36	0.456	0.740	5.614
0.75		8.33	0.449	0.733	5.635
1.00		8.29	0.441	0.724	5.670

Composition		v ₁	v ₂	v ₃	v ₄
X	Y				
0.00	0.00	556	432	----	----
0.25		572	422	341	----
0.50		581	401	----	----
0.75		590	404	340	320
1.00		585	410	326	----
0.00	0.05	550	410	350	345
0.25		562	412	364	351
0.50		580	407	335	----
0.75		588	402	343	321
1.00		596	400	359	360
0.00	0.10	547	400	375	360
0.25		569	380	366	355
0.50		588	381	369	340
0.75		584	380	360	350
1.00		598	405	361	348

Figure captions

Composition		Curie temperature in K	Activation energy in (eV)	
x	y		Ferrimagnetic region	Paramagnetic region
0.00	0.00	-	-	0.87
0.25		592	0.41	0.76
0.50		685	0.34	0.64
0.75		710	0.083	0.59
1.00		724	0.072	0.53
0.00	0.05	-	-	0.80
0.25		597	0.459	0.58
0.50		631	0.369	0.55
0.75		650	0.281	0.53
1.00		680	0.240	0.64
0.00	0.10	-	-	0.84
0.25		571	0.620	0.81
0.50		610	0.338	0.66
0.75		636	0.296	0.63
1.00		653	0.216	0.51

27. Long Kla. and Tein shouwu Chang., J. Phy. D- 4B, 13/2 (1980) 259.
28. Kararche B.R, Khasabardar B.V and VaingankarA.S., J.Mag. Mag. Mat.,168(1995)292.
29. Irkin P. Yu and Turov E .A., Fiz. Met. Metallered 4(1957) 582.
30. Thorpe J and Muhammad-Ahmed M. and Sawage C., J. Mater. Sci. Lett. 6 (1987) 1341.

References

1. J Smith and H P J Wijn, "Ferrites" Physical Properties of ferromagnetic oxides in relation to their technical applications; (Endhoven, Philips)1959, The Netherlands.
2. Jonker G.H., Phys. Grav., 22 (1956) 707
3. Viwanathan B and Murthy V.R.K., Ferrites "Materials science and technology" Narosha Publishing House, New Delhi (1990).
4. S Radhakrishna and K Badrinath., J. Mater. Sci. Lett., 3 (1984) 807
5. A B Naik and J Powar., Ind. J. Pure and Appl. Phy., 23 (1985) 436.
6. R Sathyanarayana, S Murthy, T Rao and S Rao., J. Less. Comm. Metal.,90 (1983) 243.
7. P V Reddy, K J Pratap and T S Rao., Cryst. Res. Technol. 22 (1987) 977.
8. S. A Mazen, A. Abd, El Rahiem and B Sarba., J. Mater. Sci., 23 (1988) 917.
9. S.S Suryavamshi, R S Patil and S R Sawant .,J. Less. Comm. Met., 168 (1991) 169.
10. M .A. El Hiti., J. Mag. Mag. Mater., 136 (1994) 138.
11. M .A. El Hiti., Phase transitions., 54 (1995) 117.
12. N Relescu, E Relescu, P C Pasnicu and M L Craus. J. Mag. Mag. Mat.,136 (1994) 319.
13. C. B. Kolekar, P. N .Kamble and A. S. Vaingankar., J. Mag. Mag. Mat. 38 (1994) 211.
14. N. Rezlescu, E. Rezlescu, Pasnicu and M.L, Craus., Mater. Res. Bull. 33 915 (1998).
15. R. K. Kumar and G.Srivastava., J. Appl. Phys.,70 6115 (1994).
16. B.V. Bhise, M.B. Domgar, S.A. Patil, and S.R.Sawant., J. Mater, Sci, Lett., 65 593 (1988)
17. R. D. Waldron., Phy. Rev., 99 1727 (1955).
18. O. S. Josyulu and Sobhanadri., Phys. Status. Solidi (a), 65 479 (1981).
19. El Hiti, M.A. El Shora, A.I. Seoud and S.M. Hammaed., Phase transitions 56 35 (1994).
20. R. D. Waldron, J. Phy. Eev , 99 1727 (1955).
21. O. S. Josyulu and Sobhanadri, J. Phys. Status. Solidi. (a), 65 479 (1981).
22. El Hiti, M.A. El Shora, A.I. Seoud and S.M. Hammaed, J. Phase transitions 56 35 (1994).
23. Rane K. S, Vernekar M. S. and Sawant P.Y., Bull. Mater. Sci., 5 (2001) 323.
24. Sattar A. A., Egypt. J. Sol., 26 (2003) 113.
25. D. Ravindra T. and Sheshagiri Rao., Cryst. Res. Technol., 25 (8) (1990) 963.
26. Rane K.S, Vernekar.V.M.S., Bull.Mater. Sci., 24 39. (2001)